Article No. jmbi.1999.2800 available online at http://www.idealibrary.com on IDEAL® J. Mol. Biol. (1999) 289, 579–590

JMB

Determination of the MurD Mechanism Through Crystallographic Analysis of Enzyme Complexes

Jay A. Bertrand[1]*, Geneviève Auger[2], Lydie Martin[1], Eric Fanchon[1] Didier Blanot[2], Dominique Le Beller[3], Jean van Heijenoort[2] and Otto Dideberg[1]

[1]*Institut de Biologie Structurale Jean-Pierre Ebel (CEA-CNRS), Laboratoire de Cristallographie Macromoléculaire, 41 rue Jules Horowitz, F-38027 Grenoble Cedex 1, France*

[2]*EP1088 du Centre National de la Recherche Scientifique, Biochimie Structurale et Cellulaire, Université de Paris-Sud, Orsay, France*

[3]*HMR, Groupe des Maladies Infectieuses, Service de Biochimie, 102 route de Noisy, F-93235 Romainville Cedex, France*

**Corresponding author*

UDP-*N*-acetylmuramoyl-L-alanine:D-glutamate (MurD) ligase catalyses the addition of D-glutamate to the nucleotide precursor UDP-*N*-acetylmuramoyl-L-alanine (UMA). The crystal structures of three complexes of *Escherichia coli* MurD with a variety of substrates and products have been determined to high resolution. These include (1) the quaternary complex of MurD, the substrate UMA, the product ADP, and Mg^{2+}, (2) the quaternary complex of MurD, the substrate UMA, the product ADP, and Mn^{2+}, and (3) the binary complex of MurD with the product UDP-*N*-acetylmuramoyl-L-alanine-D-glutamate (UMAG). The reaction mechanism supported by these structures proceeds by the phosphorylation of the C-terminal carboxylate group of UMA by the γ-phosphate group of ATP to form an acyl-phosphate intermediate, followed by the nucleophilic attack by the amino group of D-glutamate to produce UMAG. A key feature in the reaction intermediate is the presence of two magnesium ions bridging negatively charged groups.

Keywords: crystal structure; peptidoglycan; drug design; ADP ligase; enzymatic mechanism

Introduction

Recent concerns related to the increasing levels of antibiotic resistance have renewed efforts in the search for new antibacterial drug targets. The proteins involved in peptidoglycan biosynthesis are such possible targets. Peptidoglycan is formed as linear repeating disaccharide chains interconnected by a short peptide moiety. Four ADP-forming ligases (MurC, MurD, MurE and MurF) catalyse the assembly of the peptide moiety by successive additions of L-Ala, D-Glu, *meso*-DAP (or L-Lys), and D-Ala-D-Ala. MurD, the ADP-forming ligase that catalyses the formation of the peptide bond between UDP-*N*-acetylmuramoyl-L-alanine and D-Glu, is of particular interest because of the highly specific incorporation of D-Glu in the peptidoglycan.

In an earlier publication we reported the structure of UDP-*N*-acetylmuramoyl-L-alanine:D-glutamate ligase (MurD) from *Escherichia coli* in the presence of the substrate UDP-*N*-acetylmuramoyl-L-alanine (UMA) at 1.9 Å resolution (Bertrand *et al.*, 1997). The MurD·UMA structure revealed a three-domain protein topology and defined the UMA-binding site. Each domain of MurD is reminiscent of nucleotide-binding folds: the N and C-terminal domains are consistent with the dinucleotide-binding fold and the central domain with the mononucleotide-binding fold. The presence of a bound sulphate molecule and comparisons with known NTP-bound structures allowed a general definition of the ATP-binding site.

In order to better understand the molecular mechanism of MurD, we have extended our structural studies to include mononucleotide-bound complexes in the presence of UMA and the complex with the final product of the enzymic reaction UDP-*N*-acetylmuramoyl-L-alanine-D-glutamate (UMAG). These structures reveal valuable information relating to the first step of the MurD

Abbreviations used: MurD, UDP-*N*-acetylmuramoyl-L-alanine:D-glutamate ligase; UMA, UDP-MurNAc-L-Ala; UMAG, UDP-MurNAc-L-Ala-D-Glu; AMP-PNP, adenylylimidodiphosphate; DAP, diaminopimelate; NTP, nucleoside triphosphate; rms, root-mean-square.

E-mail address of the corresponding author: otto@ibs.fr

0022-2836/99/230579–12 $30.00/0

mechanism, phosphoryl transfer to form the acyl-phosphate intermediate, and the second step, nucleophilic attack of the acyl-phosphate intermediate. Two different procedures were used in our attempt to obtain structural information relating to the initial step of the MurD mechanism, phosphoryl transfer. In the first approach, crystals of MurD were grown from a sulphate-free solution that contained UMA, ADP, Mg^{2+}, NaF and $AlCl_3$. These crystallization conditions were chosen with the hope that trigonal AlF_3 or square AlF_4^- would form as an analogue of the γ-phosphoryl group, providing a snapshot of the transition state of the enzyme (Wittinghofer, 1997). Upon solving the structure we realized that AlF_3 was not bound in the active site. Instead, we obtained the complex MurD·UMA·ADP·Mg^{2+}, which revealed two divalent cation-binding sites and provided valuble information concerning the probable position of the γ-phosphate group of ATP. In the second approach, crystals grown in the presence of UMA and sulphate were transferred into a PEG solution that contained the divalent cation Mn^{2+} and the ATP analogue adenylylimidodiphosphate (AMP-PNP). However, while attempting to produce the enzymatic complex with AMP-PNP we obtained, instead, the hydrolysed product giving the complex MurD·UMA·ADP·Mn^{2+}.

No structural information was available concerning the second step of the MurD mechanism, nucleophilic attack on the acyl-phosphate intermediate by the amino group of D-Glu. In order to obtain structural information relating to this step of the mechanism, we have solved the structure of MurD in the presence of the reaction product UDP-*N*-acetylmuramoyl-L-alanine-D-glutamate. This study highlights the specific differences and similarities at the active site that result from ADP-binding, UMAG-binding and the addition of either manganese or magnesium.

Results and Discussion

Quality of the structures

The overall structure of MurD (Figure 1) has been described (Bertrand *et al.*, 1997). The designation of secondary structural elements that were previously adopted will be followed in this work. Strands (β) and helices (α) are denoted by numbers that relate to the order of occurrence along the polypeptide chain. The structures of the complexes MurD·UMA·ADP·Mg^{2+}, MurD·UMA·ADP·Mn^{2+} and MurD·UMAG were solved by difference Fourier methods. Initial phases were calculated from the protein coordinates of the refined MurD·UMA complex (PDB code 1UAG; Bertrand *et al.*, 1997), which has a crystallographic *R*-factor of 19.0% at 1.9 Å resolution. (Details of the structure solutions are given in Materials and Methods.)

The overall structures of the enzyme are similar to the structure of MurD·UMA, indicating that the refined complexes have a conformation similar to that of the binary complex. The overall rms deviation for main-chain atoms between the original MurD·UMA model and the complexes are 0.44 Å (MurD·UMA·ADP·Mg^{2+}), 0.33 Å (MurD·UMA·ADP·Mn^{2+}) and 0.38 Å (MurD·UMAG). No non-glycine residue was found in the disallowed regions of the Ramachandran plots (Ramachandran *et al.*, 1963) and only one residue, Phe303 in the MurD·UMA·ADP·Mg^{2+} and MurD·UMA·ADP·Mn^{2+} structures, was located in the generously allowed regions. The strained φ,ψ angles of Phe303 presumably result from the side-chain movement of the adjacent Arg302 and the reorganization of the hydrogen-bonding network that occurs in order to accommodate the ADP molecule.

Enzymatic complex with Mg^{2+} and ADP

The position of the substrate UMA is identical with that in the earlier structure, MurD·UMA (Bertrand *et al.*, 1997), and the pattern of enzyme-substrate interactions is essentially preserved. Exceptions include the loss of the hydrogen bond between His183 and one of the UMA carboxylate oxygen atoms and the role the same oxygen atom plays as a coordinating atom for the magnesium ion (Figure 2(a)). An analysis of sequence alignments using all currently available MurD sequences reveals that the amino acids involved in UMA binding are structurally conserved. One exception to the conservation is Thr36 (Figure 3), a residue that interacts with UMA through both its backbone nitrogen and O^{γ} atoms. In addition, analysis of *B*-factors and accessible surface area for UMA indicates an overall strong binding of the substrate, with the extremities serving as anchor points with lower solvent accessibility; UMA has an average B-value of 8.73 $Å^2$ and solvent accessibility values that indicate that the substrate is 88% buried. The ribose moiety in the middle of UMA shows some-

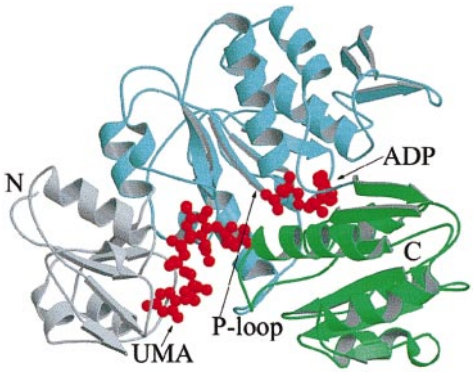

Figure 1. Overall view of the binding of UMA and ADP to MurD. The C^{α} trace of MurD is shown in grey, blue and green for the N-terminal, central and C-terminal domains, respectively. UMA and ADP are shown in red.

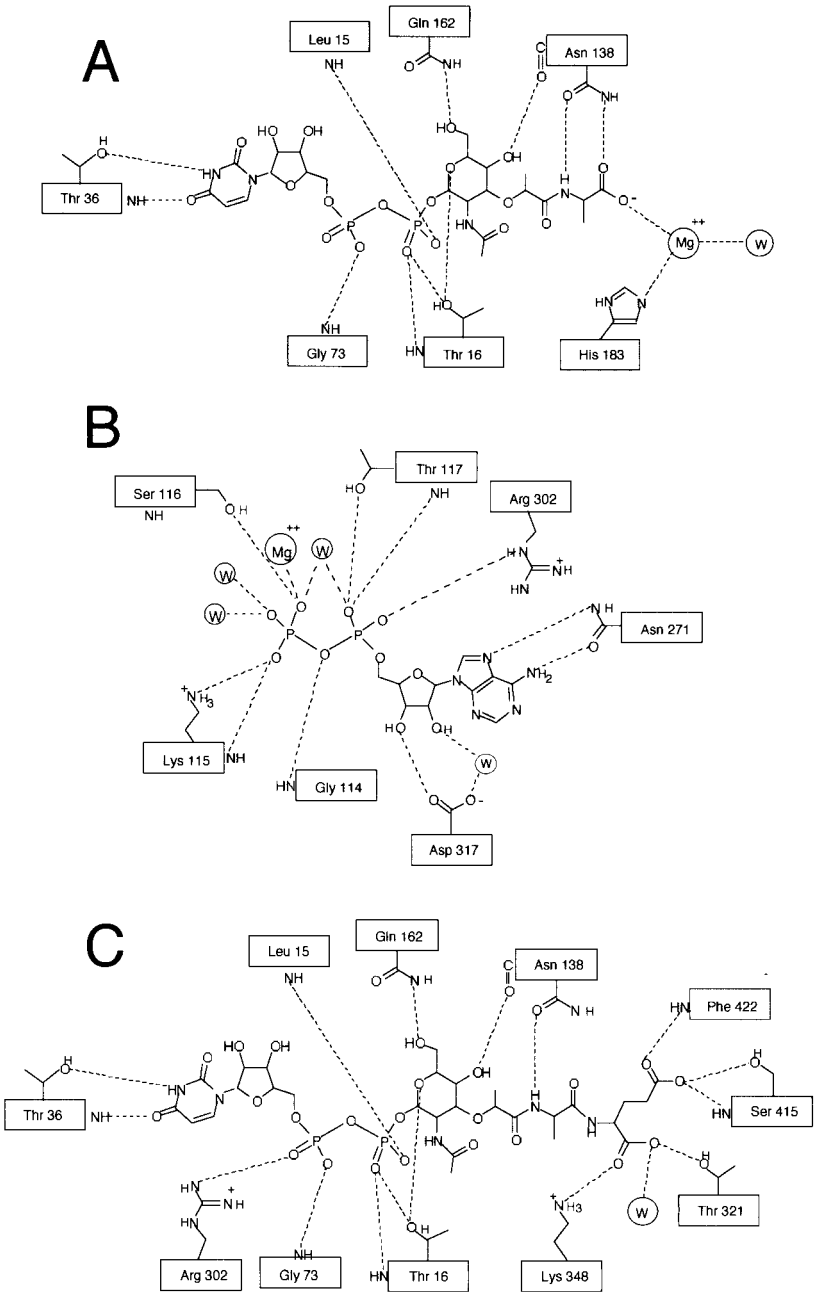

Figure 2. Schematic drawings of the (a) UMA, (b) ADP and (c) UMAG-binding sites in MurD.

what higher *B*-values and is slightly more exposed than the rest of the substrate.

As predicted from the MurD·UMA structure (Bertrand *et al.*, 1997), the ADP molecule is bound to a classical mononucleotide-binding fold, which includes the P-loop Ala-Ile-Thr-Gly-Ser-Asn-Gly-Lys-Ser (residues 108-116; Figures 1 and 3). Difference Fourier maps clearly show the entire ADP molecule bound in a pocket between the central and C-terminal domains (Figure 1). The pocket is bounded by two β-strand-to-helix switch regions (residues 108-128 and 316-330), the α10 helix (residues 266-282) and the loop that bridges the central domain to the C-terminal domain (residues 295-304). The adenine group protudes up into the central domain between helices α6 (115-228) and α10 (266-282); the pocket containing the adenine moiety is formed by Asn113 and Gly114 on one side, His267 on the other and Asn271 sits at the top. Presumably, a large component of the adenine specificity of MurD comes from the two hydrogen bonds formed between the side-chain atoms of Asn271 and adenine ring atoms N-6 and N-7 (Figures 2(b) and 5(b)), which anchor the adenine moiety in its central domain pocket. The ribose ring extends towards the C-terminal domain, forming hydrophobic interactions with Ser325 and hydrogen bonds with the side-chain of Asp317 and a conserved water molecule. The diphosphate group rests at the N terminus of helix α6 (115-128) with the α-phosphate group sitting in the anion hole and the β-phosphate group extending down

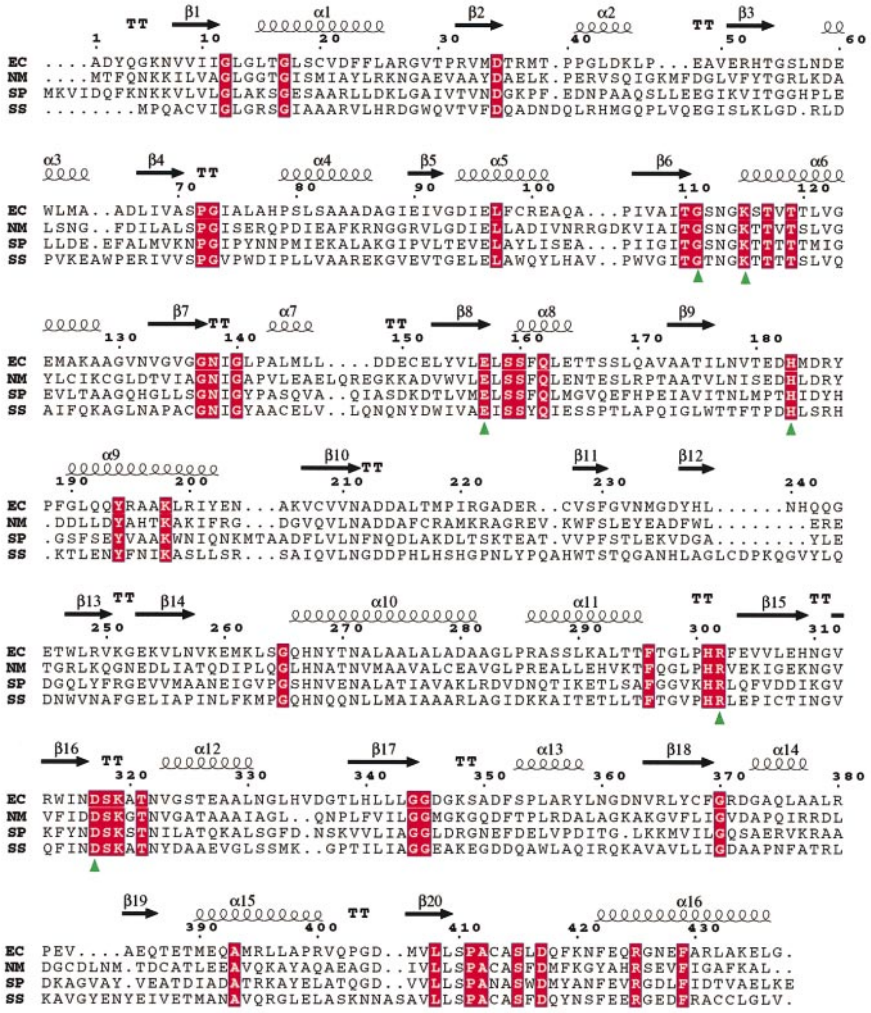

Figure 3. Sequence alignment of representative MurD ligases. The first line represents secondary structure assignment according to the program DSSP. The following lines are sequences for: EC, *Escherichia coli*; NM, *Neisseria meningitidis*; SP, *Streptococcus pneumoniae*; SS, *Synechocystis* sp. Residues that are conserved in 14 available MurD sequences and in the ADP-forming ligase superfamily are boxed and marked as green triangles, respectively. This Figure was generated by using ESPript available at the Web site www.ipbs.fr/ESPript/.

the interdomain cleft towards the carboxyl group of UMA. The α-phosphate group interacts with Gly114, Thr117 and Arg302, and the β-phosphate group with Gly114, Lys115, Ser116 and one of the magnesium ions.

The largest side-chain movement that presumably occurs as a result of binding ATP/ADP is observed for Arg302. In the MurD·UMA structure, Arg302 forms an electrostatic link with Asp317, two hydrogen bonds with Oγ of Ser325 and two hydrogen bonds with sulphate oxygen atoms (Figure 5(a) and (b)). However, in the ADP complex, none of these Arg302 interactions are present. Instead, the side-chain of Arg302 reorients itself so that it extends down the interdomain cleft parallel with the diphosphate group. Three new hydrogen bonds are made by Arg302, which include one with an oxygen atom of the α-phosphate group of ADP, one with the carbonyl oxygen atom of Pro300 and one with O^{γ} of Ser116. The side-chain of Asp317 is fixed strongly in place in both crystal structures by hydrogen bonds to the backbone nitrogen atom of Phe303, O^{γ} of Ser410 and a conserved water molecule. In the ADP complex, the electrostatic link to one of the carboxyl oxygen atoms of Asp317 that was present in the MurD·UMA structure has been replaced by a hydrogen bond with O3′ of the ADP ribose moiety. The other hydroxyl group of the ribose moeity forms a hydrogen bond with Wat508 which, in turn, hydrogen bonds with the other carboxyl oxygen atom of Asp317.

Over the course of the refinement of each complex, excess difference density at N^{ζ} of Lys198 became stronger and more clearly defined, leading to the conclusion that Lys198 had been chemically modified by the covalent addition of three atoms (Figure 4). Similar ($|F_o| - |F_c|$) density is present in the MurD·UMA complex (PDB code 1UAG; Bertrand *et al.*, 1997) although at the lower resolution and without the magnesium ion the density is of a poorer quality. As a result, no explanation has been

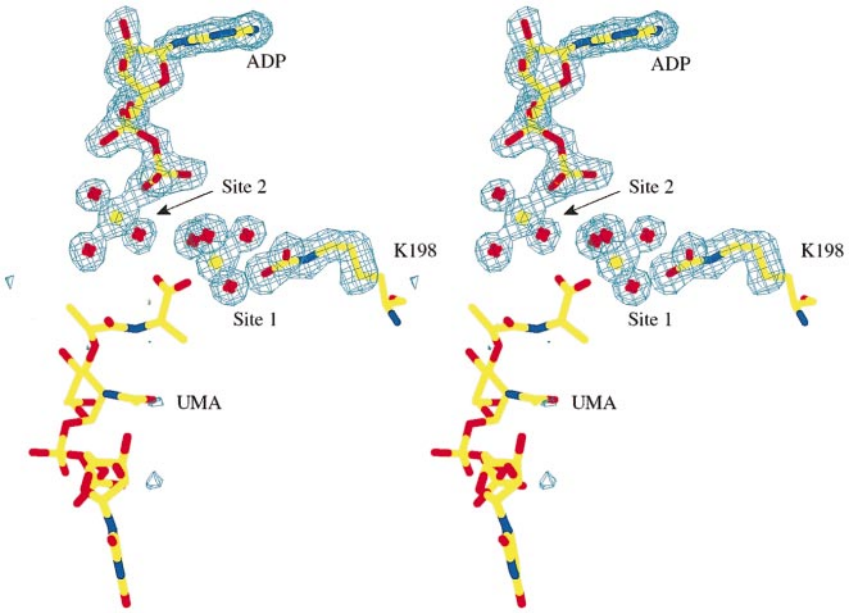

Figure 4. Stereo view of the difference electron density in the refined ($|F_o| - |F_c|$) map for the active-site region of the MurD·UMA·ADP·Mg^{2+} complex. For the structure factor calculation, Lys198 was treated as alanine, ADP, both Mg^{2+} and the ligated water molecules were excluded from the model. Water molecules and Mg^{2+} are in red and yellow, respectively. This Figure was generated by using the program O (Jones *et al.*, 1991).

previously given for this excess density. Examination of the density shows that the attached atoms are coplanar with N^{ζ} of Lys198 and that the two terminal atoms are within hydrogen-bonding distance of the backbone nitrogen atom of Ser160, the terminal hydroxyl group of Tyr194 and two water molecules that are also ligands for one of the magnesium ions. The conservation of Ser160, Tyr194 and Lys198 in all of the known MurD sequences is noteworthy (Figure 3). Since the two terminal atoms receive hydrogen bonds, they have been identified as oxygen atoms which, in turn, implies a carbamate derivative of Lys198. All three atoms of the carbamate have full occupancy and their temperature factors (7.34 $Å^2$ for C^{η}, 7.09 $Å^2$ for $O^{\eta 1}$ and 6.91 $Å^2$ for $O^{\eta 2}$) are in the same range as the other atoms in the general vicinity.

Cocrystallization of MurD in the presence of magnesium and ADP has led to the identification of an unexpected magnesium/manganese ion site (site 1) at the carboxyl end of the substrate UMA. The magnesium ion found in this site shows octahedral coordination with ligands that include one of the carboxyl oxygen atoms of UMA, N^{ε} atom of His183 and four water molecules (Figure 4). The average distance between the magnesium ion and the six coordinating atoms in its inner sphere is 2.1 Å. Interestingly, two of the four water molecules are acting as bridges between the magnesium ion and the carbamate oxygen atoms of Lys198. This finding suggests a potential role for the modified Lys198 in the formation of this magnesium/manganese ion site. Indeed, in several previously reported structures, carbamylated lysine residues have often played a role in the formation of metal-binding sites (Lundqvist & Schneider, 1991; Jabri *et al.*, 1995). However, in the reported structures the carbamate oxygen atoms are generally ligands in the first coordination sphere of the metal rather than in the second, as observed in MurD.

Many enzymes with the classical mononucleotide-binding topology also contain a divalent cation pocket, which is formed by the conserved hydroxyl residue at the last position of the P-loop and an acidic residue at the C terminus of the adjacent β-strand (Ser116 and Glu157 in MurD). This metal ion presumably occupies a site between the β and γ phosphate groups of ATP, which facilitates the phosphate transfer in the first step of the catalytic mechanism. This mode of Mg^{2+}/Mn^{2+} binding, with bidentate coordination of β and γ-phosphoryl oxygen atoms, has been observed in the crystal structures of several NTP-binding proteins with bound nucleotide or nucleotide analogue; examples include dethiobiotin synthase (Huang *et al.*, 1995), EF-Tu (Kjeldgaard *et al.*, 1993) and H-*ras*-p21 (Pai *et al.*, 1990). In the MurD·UMA·ADP·Mg^{2+} structure, this site (site 2) is indeed occupied by a magnesium ion that is octahedrally coordinated with an average metal to ligand distance of 2.1 Å. Coordinating the Mg^{2+} are three ordered water molecules, a β-phosphoryl oxygen atom from ADP, O^{γ} of Ser116 and a side-chain oxygen atom from Glu157 (Figure 5(b)).

Finally, in the MurD·UMA·ADP·Mg^{2+} structure one region of the protein backbone (residues 419-425) undergoes a significant conformational change in order to accommodate the ''classical'' magnesium ion. In the MurD·UMA structure, Phe422 is at the N terminus of the α16 helix (residues 422-437) and the side-chain extends towards the central domain. A shallow pocket formed by Lys319, Glu423 and His301 contains the phenyl ring of Phe422. However, in the ADP complex, Lys319 no longer extends down the interdomain cleft towards the

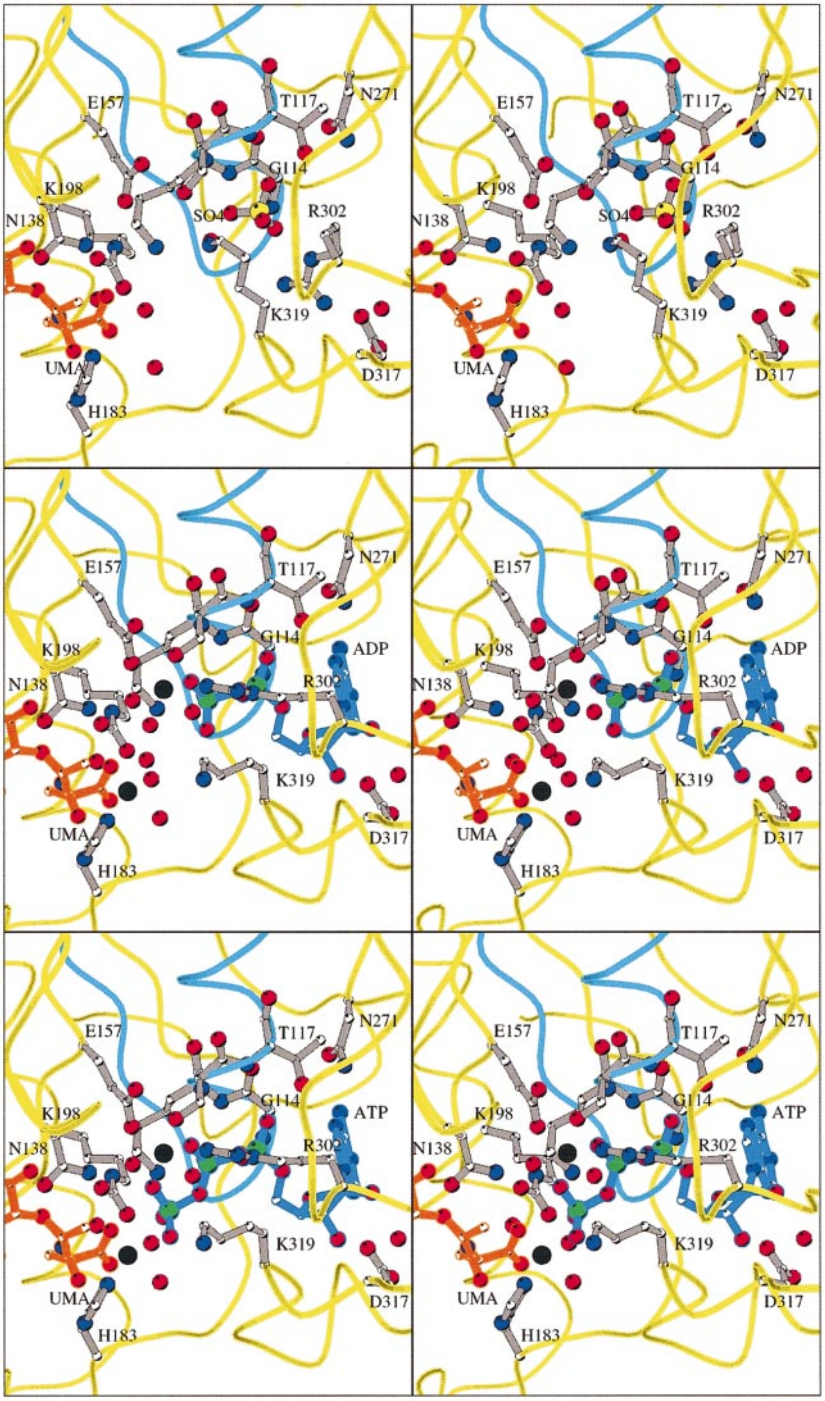

Figure 5. Stereo diagrams showing the active site: (a) (top) the MurD·UMA structure, (b) (middle) the MurD·UMA·ADP·Mg^{2+} structure and (c) (bottom) the MurD·UMA·ATP·Mg^{2+} model. The blue lines show strand β6, the P-loop and the beginning of helix α6. All important amino acid side-chains are labelled, water molecules and cations are in red and black, respectively.

active site (Figure 5(a) and (b)). Instead, it bends back through the pocket, towards the C-terminal domain. Presumably, this reorganization of the Lys319 side-chain sterically forces the shift of residues 419-425. As a result, the phenyl ring of Phe422 now extends towards the N-terminal domain, displacing several water molecules and forming hydrophobic interactions with L-Ala of UMA. In addition, the α-16 helix now begins at Glu423, since Phe422 is no longer in the helical conformation.

Enzymatic complex with Mn^{2+} and hydrolyzed AMP-PNP

Difference Fourier maps showed well-defined electron density corresponding to the ATP analogue AMP-PNP bound in the interdomain channel (not shown). No electron density was observed for the γ-phosphate group and it is believed to have been hydrolysed prior to the cryofreezing. These results are consistent with the ATPase activity that was observed when MurD was incubated with

ATP and UMA (Vaganay *et al.*, 1996). Evidence supporting the unexpected hydrolysis of imido-based nucleotide analogues has been reported for the hydrolysis of GMP-PNP by adenylosuccinate synthetase (Poland *et al.*, 1996) and AMP-PNP by the motor domain of ncd, a kinesin-related protein (Suzuki *et al.*, 1997). In the case of MurD, enzymatic hydrolysis of AMP-PNP would most likely produce adenosine-5′ (β-amino) diphosphate. However, the crystallographic data alone are unable to distinguish between the two possible products, adenosine-5′ (β-amino) diphosphate and ADP, and to unequivocally locate the position of the β-amino group. As a result, the hydrolysis product was treated as ADP during the refinement and the subsequent structural analysis.

In the MurD·UMA·ADP·Mn^{2+} complex, the binding mode and the pattern of hydrogen bonding of UMA and ADP are identical with those observed in the previous MurD·UMA·ADP·Mg^{2+} structure. In addition, a manganese ion is bound in site 1 in a manner similar to the magnesium ion of the previous stucture. One significant difference between the two quaternary structures is the lack of divalent cation occupancy in site 2, the classical site. This result was surprising, since in the previous structure site 2 was fully occupied by Mg^{2+}. Several possible explanations can be put forth for the lack of Mn^{2+} occupancy in Site2. One explanation could be related to the difference in divalent cation concentration for the two crystal structures; Mg^{2+} was present in the crystallization resevoir at a concentration of 200 mM, while Mn^{2+} was present only at 1 mM for the soakings. Another explanation could be related to the possiblity that the hydrolysis product is adenosine-5′ (β-amino) diphosphate instead of ADP and, as a result, both divalent cations might have reduced affinities for site 2. Alternatively, differences in ionic radii and Lewis acidity might explain a difference in the specificity of Mg^{2+} and Mn^{2+} for site 2. Mg^{2+} is a hard Lewis acid with a small ionic radius (0.65 Å) and therefore prefers octahedral coordination by hard Lewis bases such as oxyanions. Mn^{2+}, on the other hand, is a softer Lewis acid with a larger ionic radius (0.80 Å) and, as a result, its preference for an all-oxygen coordination is considerably less than Mg^{2+}. It is noteworthy that phosphoenolpyruvate carboxykinase, another enzyme that catalyses a phosphoryl-transfer reaction, uses a combination of Mg^{2+} and Mn^{2+} in a reaction geometry that is similar to that observed in the MurD active site (Tari *et al.*, 1997).

In the MurD·UMA·ADP·Mn^{2+} structure, one consequence of the lack of divalent cation occupancy in site 2 is that Lys319 and the loop between residues 419 and 425 are able to occupy the same positions as in the earlier MurD·UMA structure. The loop is shifted forward, covering the active site, and the side-chain of Lys319 extends down to hydrogen bond with one of the γ-phosphoryl oxygen atoms of the putative ATP. Clearly, the conformational change observed in the MurD·UMA·ADP·Mg^{2+} structure results only from the interactions between Lys319 and the metal ion in site 2, since no conformational change occurs when ADP is bound and site 2 is vacant.

Enzymatic complex with UMAG

The product UMAG binds to MurD in the cleft formed by the three domains; the UDP-*N*-acetylmuramoyl portion extends down an axis that runs between the central and C-terminal domains and the L-Ala-D-Glu portion makes a right turn toward the C-terminal domain (Figure 6). As shown in Figure 2(c), UMAG makes many polar interactions with the protein. A large number of the interactions which were observed between MurD and UMA in the previous structures are also observed for MurD and UMAG. Exceptions to this pattern are found for residues of the central domain. Presumably, the N-terminal domain residues that interact with UMA or UMAG serve a structural role and are, therefore, preserved in the UMAG complex. The central domain residues that interact with UMA in the earlier structures are Asn138, Gln162 and His183. In the MurD·UMAG structure, the positions of these residues are identical to those of the

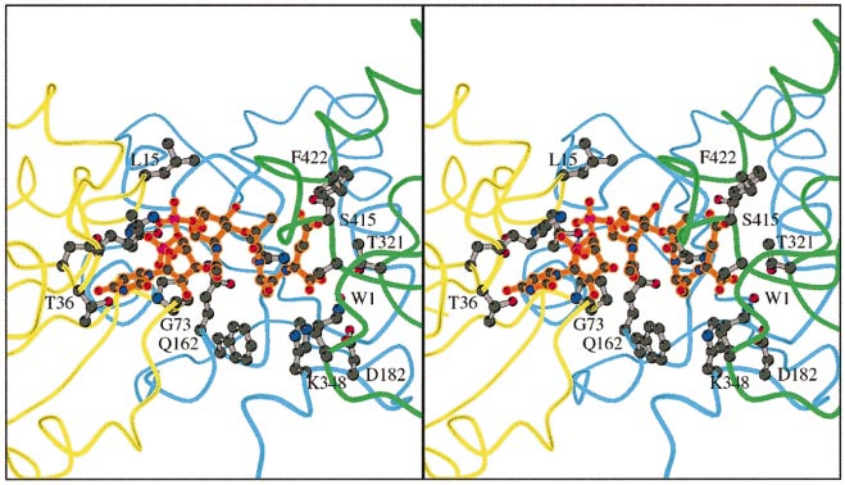

Figure 6. Stereo diagram showing UMAG bound in the cleft formed by the three domains. The C^{α} trace is shown in yellow, blue and green for the N-terminal, central and C-terminal domains, respectively. Some sections of the central domain C^{α} trace were clipped for the sake of clarity. Residues that interact with UMAG though either hydrophobic or hydrophilic interactions are shown. In the Figure, Asn138 is located behind UMAG and is unlabelled. W1 is a structurally conserved water molecule (Wat600).

earlier substrate-bound structures. However, no hydrogen bonds are made between His183 and UMAG and the pattern of hydrogen bonding has changed for Asn138. Asn138 only interacts with UMAG through $O^{\delta 1}$ and the backbone carbonyl oxygen. The hydrogen bond between $N^{\delta 2}$ of Asn138 and the carboxyl oxygen of L-Ala no longer exists after ligation of D-Glu to form UMAG. Instead, the L-Ala residue of UMAG reorients itself so that it extends toward the C-terminal domain, the location of the D-Glu binding site.

Residues from the C-terminal domain account for the D-Glu binding of UMAG (Figure 2(c) and 6). The α-carboxyl group is held in place by hydrogen bonds with N^{ζ} of Lys348, O^{γ} of Thr321, and a conserved water molecule (Wat600). Interestingly, this water molecule is one of the ligands for the site 1 divalent cation in the earlier ADP-bound structures. Furthermore, both Wat600 and N^{ζ} of Lys348 bridge between two carboxyl groups, the α-carboxyl group of D-Glu and the side-chain carboxyl group of Asp182, making an extended ring-type system. The D-Glu side-chain carboxyl group is held in place by hydrogen bonds with Ser415 and Phe422: one of its oxygen atoms hydrogen bonds with both the backbone nitrogen and the O^{γ} of Ser415, and the other with the backbone nitrogen of Phe422. The fact that Phe422 plays a role in the fixation of D-Glu is surprising based on the structural reorganization of this residue in the MurD·UMA·ADP·Mg^{2+} structure (Figure 7). Presumably, Phe422 needs to be in a helical conformation in order to interact with the D-Glu residue.

The MurD residues that interact with D-Glu of UMAG provide a specific binding site, which correlates with biochemical results for substrate specificity. This suggests that the D-Glu residue occupies the same position both before and after ligation. Using MurD from *E. coli*, Pratviel-Sosa and co-workers measured the specific activity for 24 analogues of D-Glu (Pratviel-Sosa *et al.*, 1994). Out of the 24 analogues tested only three led to specific activities over 50 %. The three substrates were, in decreasing order of substrate specificity, D-*erythro*-4-methylglutamic acid, D-*erythro*-3-methylglutamic acid and DL-homocysteic acid. Trends in the specific activities of the 24 analogues defined the essential requirements for MurD substrates. These requirements are that the α-amino acid must be in the D configuration, the side-chain needs a terminal anionic group and the two acid groups must be separated by three carbon atoms (Pratviel-Sosa *et al.*, 1994). All of these substrate requirements can be explained with relation to the D-Glu binding site in the MurD·UMAG structure (Figure 6). The geometry of the D-Glu binding site dictates the allowable distance between the two carboxyl groups. In order for both to be able to properly interact with the correct geometry they need to be separated by a fixed distance which corresponds to a distance of four carbon-carbon bonds. Next, the location of the MurD residues that interact with the side-chain carboxyl group of the D-Glu, Ser415 and Phe422, are at or near the N terminus of helix α16 and the helix dipole would presumably balance the negative charge of the anionic group. Finally, the D configuration of the α-carbon atom would position the amide nitrogen in the general vicinity of the UMA carboxyl carbon atom, the site of nucleophilic attack.

During the MurD·UMAG refinement, a difference density was observed in the active site, close to the classical Mg^{2+} site. The general form and location of the density suggest a small organic molecule that is capable of forming hydrogen bonds to several of the surrounding atoms from UMAG and the protein. However, none of the components present in the crystallization or cryoprotectant solutions fits well in the density. Based on this finding, eight dummy atoms were built into the density. After several cycles of refinement the positions of the dummy atoms converged to their final positions. In comparing these positions with those of water molecules in the previous structures, it is apparent that several of these dummy atoms occupy conserved water positions. This result and the inability to fit an organic molecule into the density has led to the hypothesis that the dummy

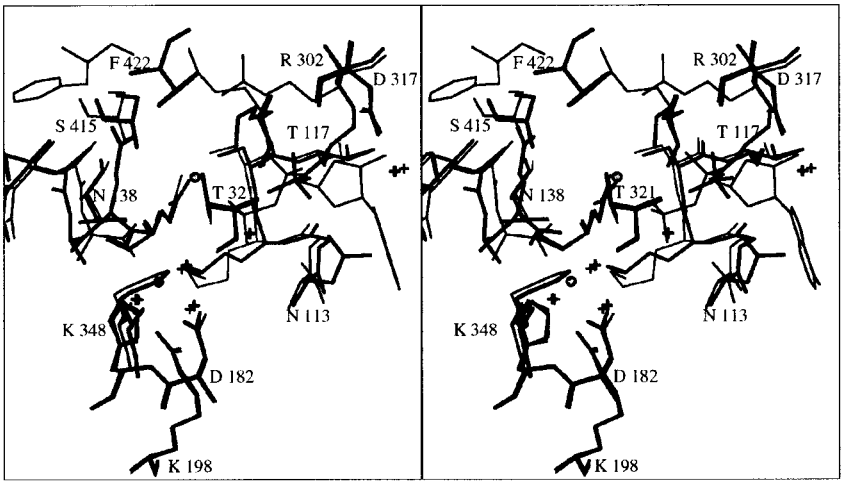

Figure 7. Superposition of the binding site of MurD·UMAG onto MurD·UMA·ADP·Mg^{2+}. The MurD·UMAG and MurD·UMA·ADP·Mg^{2+} complexes are represented in thick and thin lines, respectively. The water molecules are drawn as crosses and Mg^{2+} as circles.

atoms represent a mixture of partially occupied water molecules. Nonetheless, the dummy atoms remain in the structure at full occupancy to indicate potential atom positions.

Mechanism of MurD

The MurD reaction can be divided into three bond making/breaking steps. The first step is the initial phosphorylation of the UMA carboxylate to form the acyl-phosphate. Biochemical evidence supporting the acyl-phosphate reaction intermediate include molecular isotope exchange and TLC experiments (Vaganay *et al.*, 1996). The second step of the reaction is nucleophilic attack by the amine of D-Glu, producing a tetrahedral intermediate. The effectiveness of tetrahedral phosphinate MurD inhibitors (Tanner *et al.*, 1996; Gegnas *et al.*, 1998), analogues of UMAG, supports the existence of the tetrahedral transition-state intermediate. In the last step, the tetrahedral intermediate collapses to yield UMAG, ADP and inorganic phosphate. Figure 8 shows the reaction mechanism, which can be deduced from all the MurD structures reported here.

Analysis of the two ADP-bound structures reveals information relating to the first step, formation of the acyl-phosphate intermediate. The complexes have identified the ADP-binding site and two divalent cation sites. Presumably, both divalent cations play a critical role in the enzymatic mechanism. Prior to these structures, the cation dependency of MurD for Mg^{2+} and Mn^{2+} had been reported (Nathenson *et al.*, 1964; Pratviel-Sosa *et al.*, 1991) but no information was available concerning the required stoichiometry. The structural results identify MurD as yet another enzyme that requires two divalent cations for the phosphoryl transfer between two anionic substrates. Other examples include ADP-forming ligases such as D-Ala-D-Ala ligase (Shi & Walsh, 1995; Fan *et al.*, 1997) and glutathione synthetase (Hara *et al.*, 1996).

Although no information was obtained concerning the exact position of the γ-phosphate of ATP several conclusions may be made based on an approximate position which results from modeling using the known position of ADP and the allowed torsion angles for ATP. By analogy with other nucleotide-bound structures that share the mononucleotide-binding topology, one of the γ-phosphoryl oxygen atoms can be confidently positioned as a ligand for the Mg^{2+} in the classical cation pocket (site 2). Next, keeping in mind that the conserved lysine of the P-loop (Lys115) usually coordinates to the β and γ-phosphoryl groups, a second phosphoryl oxygen can be positioned so that it coordinates with N^{ζ} of Lys115. This placement of the second phosphoryl oxygen also makes it a ligand for the magnesium/manganese ion in site 1, displacing one of the water molecules. The combination of requirements, two γ-phosphoryl oxygen atoms that are ligands for two different divalent cations and the range of allowed torsion angles for ATP, essentially "fix" the position of the γ-phosphate (Figure 5(c)).

Assuming the γ-phosphate is correctly positioned in our model, the relative geometries of ATP and UMA suggest a direct Sn2 displacement of the γ-phosphate by the carboxyl oxygen of UMA. Structural evidence supporting the Sn2 displacement include: (i) the neutralization of the charge repulsions by Lys115 and both divalent cations; (ii) the

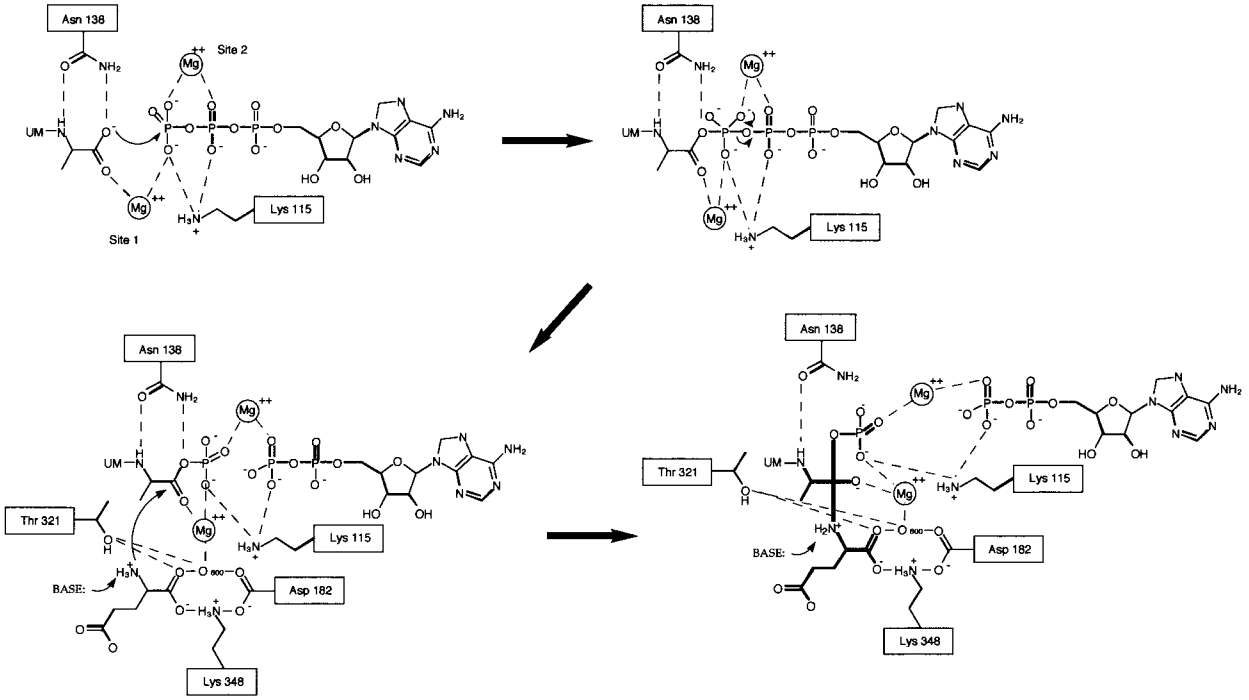

Figure 8. Proposed reaction mechanism for the synthesis of UMAG by *E. coli* MurD. Only Mg^{2+} and amino acid side-chains involved in the mechanism are included.

position of the γ-phosphate, which minimizes the interatomic distance (approximately 2.2 Å) and directs the carboxyl oxygen of UMA towards the phosphorus atom in the centre of the phosphoryl tetrahedron; (iii) the activation of the carbonyl oxygen through interactions with the divalent cation in site 1; and (iv) the repulsion between the β and γ-phosphates which results from the eclipsed positions of the phophoryl oxygen atoms.

After transfer, the acyl-phosphate intermediate would be stabilized by interactions with N^{ζ} of Lys115 and the divalent cations in site 1 and site 2. Nucleophilic attack would occur after D-Glu was bound and properly oriented by the interactions with the backbone nitrogen of Phe422, O^{γ} and the backbone nitrogen of Ser415, $O^{\gamma 1}$ of Thr321, N^{ζ} of Lys348 and Wat600. Asp182 would play a role in orienting and stabilizing D-Glu through a ring-like geometry made by bridging N^{ζ} of Lys348 and Wat600 between the two carboxyl groups. The formation of the tetrahedral adduct requires a catalytic base to abstract the proton from the D-Glu amine. A few possibilities could be suggested: in the first D-Glu binds from solution in a free base form, in the second the deprotonation is assisted by the γ-phosphate of ATP bound to UMA. Finally, the transformation of the tetrahedral adduct into the final product needs another catalytic base to remove the second proton. From the MurD·UMAG complex (Figure 6) only His183 is in the vicinity (4.21 Å) of the nitrogen.

In conclusion, the structure of three MurD complexes reveals, for the first time, the active site architecture of the enzyme and the position of the molecules participating in the enzymatic reaction: UMA, ATP, Mg^{2+} and D-Glu. Residues identified by sequence analysis and the roles played by these residues in the MurD complexes substantiate a mechanism already proposed for other ADP-forming ligases. Further work implies the study of the critical amino acid residues by site-directed mutagenesis, as recently accomplished with the MurC synthetase (Bouhss *et al.*, 1997).

Materials and Methods

The MurD preparation used here was purified from *E. coli* JM83(pMLD58) as described. All crystal forms of MurD presented here were grown at 15 °C using the hanging drop method and all X-ray data were collected under cryogenic conditions at 100 K. All three enzymatic complexes gave crystals that are isomorphous with those of the original complex in ammonium sulphate (Auger *et al.*, 1998), belong to space group $P4_1$ and contain one molecule per asymmetric unit.

Preparation of the complex MurD·UMA·ADP·Mg^{2+}

Crystals of the MurD·UMA·ADP·Mg^{2+} complex were grown by equally mixing the protein (9.8 mg/ml MurD, 1 mM UMA, 5 mM ADP, 1 mM NaN_3, 1 mM DTT, 20 mM Hepes pH 7.5) with reservoir solution (12-14 % (w/v) monodisperse PEG 3350, 50 mM NaF, 5 mM $AlCl_3$, 200 mM $MgCl_2$, 100 mM Hepes pH 7.0). A single crystal was frozen for data collection using 20 % (v/v) glycerol as a cryoprotectant.

Preparation of the complex MurD·UMA·ADP·Mn^{2+}

Crystals of MurD in the presence of the substrate UMA were grown as described previously (Auger *et al.*, 1998) by mixing equal volumes of protein (9.8 mg/ml MurD, 1 mM UMA, 1 mM NaN_3, 1 mM DTT, 20 mM Hepes pH 7.5) and reservoir solution (1.6 to 1.8 M ammonium sulphate, 100 mM Hepes pH 7.2) solutions. Crystals of the desired enzymatic complex (MurD·UMA·ADP·Mn^{2+}) were produced using a slightly modified version of a crystal soaking procedure which replaces ammonium sulphate with PEG 4000 (Ray *et al.*, 1991). In the first step, crystals were soaked for thirty minutes in a solution containing 1.3 M sodium sulphate and 100 mM Hepes (pH 7.2). Next, the crystals were soaked in a solution containing 35 % PEG 4000, 120 mM sodium sulphate and 100 mM Hepes (pH 7.2). Finally, crystals were soaked for one hour in a solution containing 27 % PEG 4000, 20 % PEG 400, 1 mM AMP-PNP, 1 mM $MnCl_2$ and 100 mM Hepes (pH 7.2). After the final transfer, a single crystal was flash-frozen at 100 K in a stream of dry nitrogen produced by a cryogenic system (Oxford cryosystems) and stored in a reservoir of liquid nitrogen.

Synthesis of UMAG

D-Glutamic acid was added to UMA (Auger *et al.*, 1998) in a reaction catalysed by MurD. A mixture (24 ml) containing 0.5 mM UMA, 1 mM D-Glu, 5 mM ATP, 0.5 M Tris-HCl (pH 8.6), and enzyme (400 units) was incubated for five hours at 37 °C. More enzyme (400 units) was added, and the reaction was allowed to proceed for four additional hours. Next, the mixture was boiled for three minutes and centrifuged, and the supernatant was lyophilized. The product was purified on a column of Sephadex G-25 (fine; 80 cm × 1.6 cm) equilibrated with water. Detection at 262 nm showed that UMAG was eluted first, followed by ATP/ADP. 11.9 μmol of HPLC-pure UMAG were recovered (yield: 99 %). Amino acid analysis of an acid hydrolysate gave the results: Glu, 1.07; Ala, 1.00.

Preparation of the complex MurD·UMAG

Crystals of MurD in the presence of the reaction product UMAG were grown from ammonium sulphate as described (Auger *et al.*, 1998) with UMAG replacing UMA in the crystallization conditions. Neither ADP or ATP analogues were included in the crystallization.

Data collection and reduction

X-ray diffraction data of MurD·UMA·ADP·Mg^{2+} were collected on the D2AM beamline (ESRF, Grenoble, France) equipped with a XRII-CCD detector (Moy, 1994). X-ray data from the XRII-CCD detector were indexed, integrated and scaled using XDS (Kabsch, 1988). X-ray diffraction data of MurD·UMA·ADP·Mn^{2+} and MurD·UMAG were collected on EMBL beamlines (EMBL-BW7B, DESY, Hamburg, Germany, and EMBL-BL19, ESRF, Grenoble, France, respectively) which were equipped with MarResearch image plate scanners. X-ray data from the MarResearch detector were indexed and integrated using the program DENZO and scaled using

Table 1. MurD data collection and refinement statistics

Crystal form:	MurD·UMA·ADP·Mg^{2+}	MurD·UMA·ADP·Mn^{2+}	MurD·UMAG
Cell constants			
$a = b$ (Å)	65.6	65.2	65.8
c (Å)	136.0	134.4	134.5
Data collection			
X-ray source	D2AM (ESRF)	BW7B-EMBL (DESY)	BL19-EMBL (ESRF)
Wavelength (Å)	1.073	0.881	0.978
d_{min} (Å)	1.69	1.77	1.66
No. of unique	61,463	54,268	66,314
Multiplicity	5.5	4.6	4.6
Completeness (%)	96.0 (78.8)	99.2 (98.7)	98.4 (85.3)
$\langle I/\sigma(I)\rangle$	36.7 (9.0)	25.6 (8.6)	32.9 (10.8)
Overall B (Å^2)	12.6	14.9	16.8
R_{sym} (%)	8.1 (29.4)	6.6 (20.4)	4.1 (14.9)
Refinement			
Resolution range (Å)	8.0-1.70	8.0-1.77	8.0-1.66
$R_{crystal}$ (%)	18.0	17.8	19.0
R_{free} (%)	20.6	22.2	22.6
Avg. B-value (Å^2)/No. of non-hydrogen atoms			
Protein	12.64/3231	15.75/3235	14.28/3230
Backbone	11.19/1717	14.46/1721	12.90/1717
UMA/UMAG	8.73/49	11.92/49	16.16/58
ADP/SO_4	7.32/27	11.40/27	11.90/5
Water molecules	26.25/431	27.81/359	25.93/322
Mg^{2+}/Mn^{2+}	6.28/2	12.75/1	
Other		30.86/15 (Hepes)	35.05/8 (dummy)
Total	14.12/3740	16.91/3686	16.62/3662

Numbers in parentheses correspond to the shell of data at highest resolution: 1.72-1.69 Å for MurD·UMA·ADP·Mg^{2+}, 1.83-1.77 Å for MurD·UMA·ADP·Mn^{2+} and 1.72-1.66 Å for MurD·UMAG.

the program SCALEPACK (Otwinowski & Minor, 1997). All structure factor amplitudes were calculated using the program TRUNCATE of the CCP4 program package (CCP4, 1994). Details of the data collection and processing for the synchrotron cryo-data are given in Table 1.

Crystallographic refinement

Refinement was performed with X-PLOR (Brünger, 1992b) using the refined protein coordinates of the MurD·UMA complex (PDB code: 1UAG; Bertrand *et al.*, 1997) as a starting model. A 5% subset of the reflections was randomly chosen to monitor R_{free} (Brünger, 1992a). The models were refined using an intial cycle of rigid-body and conventional positional refinement. Next a round of refinement was performed with the protein model which included simulated annealing, conventional positional refinement, and individual B-factor refinement. Subsequent rounds of refinement included conventional positional refinement and individual B-factor refinement followed by manual inspection of the electron density maps using the program O (Jones *et al.*, 1991). Molecules and ions were located and built into the density over the course of the refinement. Prior to the last cycle of refinement an anisotropic correction was made on the reflections using X-PLOR (Brünger, 1992b).

While refining the different structures, excess ($|F_o| - |F_c|$) density at the N^{ζ} atom of Lys198 became stronger and more clearly defined over the course of the refinement. This density was attributed to a carbamate derivative of Lys198 (see Results and Discussion). The final results of the refinement are given in Table 1.

Figures 1, 5, 6, 7 were generated by using MOLSCRIPT (Kraulis, 1991).

Accession numbers

The structures of the three complexes have been deposited with the Protein Data Bank (MurD·UMA·ADP·Mg^{2+}, accession number 2UAG; MurD·UMA·ADP·Mn^{2+}, accession number 3UAG, MurD·UMAG, accession number 4UAG).

Acknowledgements

This is Publication n° 610 of the Institut de Biologie Structurale Jean-Pierre Ebel (CEA-CNRS). We are grateful to Dr A. D'Arcy for providing information that led to the crystallisation of MurD·UMA·ADP·Mg^{2+} using monodisperse PEG3350 and S. Thieffine for help with the Figures. We thank DESY (Hamburg) and ESRF (Grenoble) for access to synchrotron radiation, in particular V. Lamzin (BW7B), M. Roth (D2AM) and A. Thompson (BL19) for generous help during data collection. This work was supported by grants from the Action Concertée Coordonnée, Sciences du Vivant (N° V).

References

Auger, G., Martin, L., Bertrand, J., Ferrari, P., Fanchon, E., Vaganay, S., Pétillot, Y., van Heijenoort, J., Blanot, D. & Dideberg, O. (1998). Large-scale preparation, purification, and crystallization of UDP-*N*-acetylmuramoyl-L-glutamate ligase from *Escherichia coli*. *Protein Expr. Purif.* **13**, 23-29.

Bertrand, J. A., Auger, G., Fanchon, E., Martin, L., Blanot, D., van Heijenoort, J. & Dideberg, O. (1997).

Crystal structure of UDP-*N*-acetylmuramoyl-L-alanine:D-glutamate ligase from *Escherichia coli*. *EMBO J.* **16**, 3416-3425.

Bouhss, A., Mengin-Lecreulx, D., Blanot, D., van Heijenoort, J. & Parquet, C. (1997). Invariant amino acids in the Mur peptide synthetases of bacterial peptidoglycan synthesis and their modification by site-directed mutagenesis in the UDP-MurNAc: L-alanine ligase from *Escherichia coli*. *Biochemistry,* **36**, 11556-11563.

Brünger, A. T. (1992a). Free *R* value: a novel statistical quantity for assessing the accuracy of crystal structures. *Nature,* **355**, 472-475.

Brünger, A. T. (1992b). *X-PLOR Version 3. 1: A System for X-ray Crystallography and NMR*, Yale University Press, New Haven, CT.

CCP4, (1994). The CCP4 suite: programs for protein crystallography. *Acta Crystallog. sect. D,* **50**, 760-763.

Fan, C., Park, I-S., Walsh, C. T. & Knox, J. R. (1997). D-alanine:D-alanine ligase: phosphonate and phosphinate intermediates with wild type and the Y216F mutant. *Biochemistry,* **36**, 2531-2538.

Gegnas, L. D., Waddell, S. T., Chabin, R. M., Reddy, S. & Wong, K. K. (1998). Inhibitors of the bacterial cell wall biosynthesis enzyme MurD. *Bioorg. Med. Chem. Letters,* **8**, 1643-1648.

Hara, T., Kato, H., Katsube, Y. & Oda, J. (1996). A pseudo-Michaelis quaternary complex in the reverse reaction of a ligase: structure of *Escherichia coli* B glutathione synthetase complexed with ADP, glutathione, and sulfate at 2.0 Å resolution. *Biochemistry,* **35**, 11967-11974.

Huang, W., Jia, J., Gibson, K. J., Taylor, W. S., Rendina, A. R., Schneider, G. & Lindqvist, Y. (1995). Mechanism of an ATP-dependent carboxylase, dethiobiotin synthetase, based on crystallographic studies of complexes with substrates and a reaction intermediate. *Biochemistry,* **34**, 10985-10995.

Jabri, E., Carr, M. B., Hausinger, R. P. & Karplus, P. A. (1995). The crystal structure of urease from *Klebsiella aerogenes*. *Science,* **268**, 998-1004.

Jones, T. A., Zou, J.-Y., Cowan, S. W. & Kjeldgaard, M. (1991). Improved methods for building protein models in electron density maps and the location of errors in these models. *Acta Crystallog. sect. D,* **47**, 110-119.

Kabsch, W. (1988). Evaluation of single crystal X-ray diffraction data from a position sensitive detector. *J. Appl. Crystallog.* **21**, 916-924.

Kjeldgaard, M., Nissen, P., Thirup, S. & Nyborg, J. (1993). The crystal structure of elongation factor EF-Tu from *Thermus aquaticus* in the GTP conformation. *Structure,* **1**, 35-50.

Kraulis, P. J. (1991). MOLSCRIPT: a program to produce both detailed and schematic plots of protein structures. *J. Appl. Crystallog.* **24**, 946-950.

Lundqvist, T. & Schneider, G. (1991). Crystal structure of activated ribulose-1,5-bisphosphate carboxylase complexed with its substrate, ribulose-1,5-bisphosphate. *J. Biol. Chem.* **266**, 12604-12611.

Moy, J.-P. (1994). A 200 mm input field, 5-80 keV detector based on an X-ray image intensifier and CCD camera. *Nucl. Instrum. Meth. Phys. Res. sect. A,* **348**, 641-644.

Nathenson, S. G., Strominger, J. L. & Ito, E. (1964). Enzymatic synthesis of the peptide in bacterial uridine nucleotides. IV. Purification and properties of the D-glutamic acid-adding enzyme. *J. Biol. Chem.* **239**, 1773-1776.

Otwinowski, Z. & Minor, W. (1997). Processing of X-ray diffraction data collected in oscillation mode. In *Methods in Enzymology* (Carter, C. W., Jr & Sweet, R. M., eds), vol. 276, pp. 307-326, Academic Press, New York, USA.

Pai, E. F., Krengel, U., Petsko, G. A., Goody, R. S., Kabsch, W. & Wittinghofer, A. (1990). Refined crystal structure of the triphosphate conformation of H-*ras*-p21 at 1.35 Å resolution: implications for the mechanism of GTP hydrolysis. *EMBO J.* **9**, 2351-2359.

Poland, B. W., Hou, Z., Bruns, C., Fromm, H. J. & Honzatko, R. B. (1996). Refined crystal structures of guanine nucleotide complexes of adenylosuccinate synthetase from *Escherichia coli*. *J. Biol. Chem.* **271**, 15407-15413.

Pratviel-Sosa, F., Mengin-Lecreulx, D. & van Heijenoort, J. (1991). Over-production, purification and properties of the uridine diphosphate *N*-acetylmuramoyl-L-alanine:D-glutamate ligase from *Escherichia coli*. *Eur. J. Biochem.* **202**, 1169-1176.

Pratviel-Sosa, F., Acher, F., Trigalo, F., Blanot, D., Azerad, R. & van Heijenoort, J. (1994). Effect of various analogues of D-glutamic acid on the D-glutamate-adding enzyme from *Escherichia coli*. *FEMS Microbiol. Letters,* **115**, 223-228.

Ramachandran, G. N., Ramakrishnan, C. & Sasisekharan, V. (1963). Stereochemistry of polypeptide chain configurations. *J. Mol. Biol.* **7**, 95-99.

Ray, W. J., Jr, Bolin, J. T., Puvathingal, J. M., Minor, W., Liu, Y. W. & Muchmore, S. W. (1991). Removal of salt from a salt-induced protein crystal without cross-linking. Preliminary examination of ''desalted'' crystals of phosphoglucomutase by X-ray crystallography at low temperature. *Biochemistry,* **30**, 6866-6875.

Shi, Y. & Walsh, C. T. (1995). Active site mapping of *Escherichia coli* D-Ala-D-Ala ligase by structure-based mutagenesis. *Biochemistry,* **34**, 2768-2776.

Suzuki, Y., Shimizu, T., Morii, H. & Tanokura, M. (1997). Hydrolysis of AMPPNP by the motor domain of ncd, a kinesin-related protein. *FEBS Letters,* **409**, 29-32.

Tanner, M. E., Vaganay, S., van Heijenoort, J. & Blanot, D. (1996). Phosphinate inhibitors of the D-glutamic acid-adding enzyme of peptidoglycan biosynthesis. *J. Org. Chem.* **61**, 1756-1760.

Tari, L. W., Matte, A., Goldie, H. & Delbaere, L. T. (1997). Mg^{2+}-Mn^{2+} clusters in enzyme-catalyzed phosphoryl-transfer reactions. *Nature Struct. Biol.* **4**, 990-994.

Vaganay, S., Tanner, M. E., van Heijenoort, J. & Blanot, D. (1996). Study of the reaction mechanism of the D-glutamic acid-adding enzyme from *Escherichia coli*. *Microb. Drug Resist.* **2**, 51-54.

Wittinghofer, A. (1997). Signaling mechanistics: aluminum fluoride for molecule of the year. *Curr. Biol.* **7**, R682-R685.

Edited by R. Huber

(Received 4 February 1999; received in revised form 8 April 1999; accepted 12 April 1999)